Ke Wang, Hual-Te Chien, Thomas W. Elmer, William P. Lawrence, David M. Engel, Shuh-Haw Sheen, "Development of ultrasonic waveguide techniques for under-sodium viewing", *NDT & E International*, Volume 49, July 2012, Pages 71-76, ISSN 0963-8695, 10.1016/j.ndteint.2012.03.006.

(http://dx.doi.org/10.1016/j.ndteint.2012.03.006)

Keywords: Ultrasonic; Waveguide; In-service inspection; Sodium-cooled fast reactor; Under-sodium viewing

Development of Ultrasonic Waveguide Techniques for Under-Sodium Viewing

Ke Wang, Hual-Te Chien, Thomas W. Elmer, William P. Lawrence, David M. Engel, and Shuh-Haw Sheen

Sensors and Instrumentation Section
Nuclear Engineering Division
Argonne National Laboratory, Argonne, IL, 60439

Abstract

An ultrasonic imaging system based on waveguide techniques was developed to provide in-service inspection of reactor core of a sodium-cooled fast reactor (SFR) and potential applications in other hostile environments. By using ultrasonic waveguide techniques, we overcome the major technical challenge in developing an under-sodium viewing (USV) system that can withstand the high-temperature and corrosive environment. The chosen design of the prototype waveguide (WG) is a hybrid of bundle and spiraled-sheet WG. The prototypes show high detection sensitivity with minimal background noise by effectively reducing spurious echoes and mode conversions. Tests on prototype waveguide transducers were conducted in liquid sodium up to 340°C (650°F). C-scan images of the targets were successfully developed from both time-of-flight and amplitude variations of the reflected echoes. The ultrasonic waveguide imaging system demonstrates a capability of detecting defects with 1mm width and 0.5mm depth under molten sodium.

Keywords: Ultrasonic; Waveguide; In-service inspection; Sodium-cooled fast reactor; Under-sodium Viewing

1. Introduction

As the next generation nuclear energy systems, Generation IV reactors have been stressed by a broad range of nations and users. Their comparative advantages include reduced capital cost, enhanced nuclear safety, and minimal generation of nuclear waste [1-3]. The main contenders with past operating history are advanced liquid metal reactors (LMRs) and molten salt reactors (MSRs). Prominent systems in the former category include sodium-cooled fast reactor (SFR) and lead-cooled fast reactor (LFR), and a prominent system in the second category is liquid fluoride thorium reactor (LFTR) [4, 5].

The use of liquid metal or molten salt provides higher power density and lower operating pressure, but also brings in great challenges for the safety inspection of reactors. Visual techniques are impossible because of the opacity of the media. Electromagnetic methods are also significantly limited due to the nature of metal and salt ions in molten state. One technique that has attracted considerable attention for both defect inspection and visualization applications is ultrasonics. This technique is capable of in-situ monitoring core components to avoid loading errors, inspecting and locating loose or lost parts, and detecting defects, such as cracks, deformation, etc [6, 7].

The major challenge in developing an under-sodium viewing (USV) system is the design of a transducer that can sustain high temperature, high radiation and corrosive environment. Two major approaches being pursued are high-temperature immersion transducers and waveguide transducers [8-11]. Most of the early works were focused on development of high-temperature immersion transducers [12-14]. However, their applications in SFR have been limited because of thermal and radiation damage on the piezoelectric element and bonding material of the transducer, especially when the operating temperature is higher than the Curie temperature of the piezoelectric material. Waveguide transducer is a promising alternative approach for under-sodium viewing. The waveguide acts as a buffer rod that isolates the sensing transducer from a high-temperature and radioactive medium. Because the transducer is kept in a relatively cool environment, below the Curie temperature of its piezoelectric element, it would perform with better reliability. Furthermore, the waveguide design is more suitable for applications with space constraints, and in general the cost of a lead zirconate titanate (PZT) transducer is lower than that of a high-temperature transducer.

As defined in ASME SEC. XI [15], the resolution obtained by the optical inspection method using fiber optics must be able to distinguish 0.8 mm-wide slits at interval of 0.8 mm. In order to achieve better resolution or at least comparable resolution, we developed a USV system based on novel ultrasonic waveguide transducers (UWT). The chosen designs demonstrate high detection sensitivity with minimal background noise. Several prototypes of UWT with different lengths were constructed and tested in water and liquid sodium. C-scan images of a target, both the time-of-flight (TOF) and amplitude, were successfully generated from the reflected echoes. The UWT imaging system is capable of detecting defects with 1mm wide and 0.5mm deep under molten sodium up to 650°F.

2. Experimental Setup and Signal Processing

2.1 Under-Sodium Viewing System

Fig.1 (a) and (b) show the experimental setup and schematic diagram of the under-sodium viewing system, respectively. It was developed to evaluate the performance of the prototype UWT in molten sodium. The whole system consists of three major sections: 1) signal generation and data acquisition, which contains a signal generator and receiver (Panametrics 5058PR), a LeCroy oscilloscope (Model 9370), and a data acquisition computer with a NI-Scope board (National Instruments PCI-5124); 2) xy-scanning system, which include two motor stages and a control module (Parker 6K4); 3) sodium loop with temperature control, which consists of a test tank with opening for UWT and target, a dump tank, and temperature control modules. The scanning stages and data acquisition are controlled by a LabVIEW™ virtual instrument (VI) program and data and image analysis are conducted by MATLAB®.

Fig. 1. Under-sodium viewing system: (a) experimental setup and (b) schematic drawing

2.2 Argonne National Laboratory (ANL) UWT

The UWT under development consists a 5 MHz lead zirconate titanate (PZT) piezoelectric transducer (Aero Tech) and a waveguide (WG). Because of the high-temperature application, dry coupling between transducer and WG is preferred. Gold and indium foil are two recommended coupling materials and gold foil was used in our tests. The design of WG plays a critical role in determining the performance of UWT, especially the signal to noise ratio (S/N). The ideal UWT should have high efficiency as a transmitter and high sensitivity as a receiver. In practice, the problem with using a WG to transmit ultrasonic waves is the presence of spurious echoes resulting from wave dispersion, reverberation, mode conversion, and diffraction within the WG. Elimination or reduction of the spurious echoes is the main challenge in WG development.

The prototype WG is a hybrid that is composed of bundle-rod and spiraled-sheet WG designs, 35% thin rod and 65% shim stock, as shown in Fig. 2. The chosen design consists of four primary parts: an outer tube, shim stock , an inner tube, and a bundle of thin rods. Fabrication requires wrapping the shim stock around the inner tube and filling the tube with thin rods. The WG ends are then fill-welded and then machined to flat and parallel or with curvature to provide a focal length as required. For faster and better surface wetting, the focus lens is plated with gold [16]. Various WG length is available for different applications. Three different length, 6″, 12″, and 18″, of UWT have been fabricated and evaluated. Fig. 2 shows a UWT with 12″ WG.

For imaging purpose, the UWT is moved over the target at adjustable height so that the reflected echoes can be collected. Each echo is able to define one point on the target. The height information can be calculated from the time-of-flight (TOF) of the reflected echo. The relative position coordinates in *x*-*y* plane can be accurately recorded using the stage control software (LabVIEW^{TM}).

Fig. 2. ANL 12″ (304.8 mm) prototype UWT with bundle-rod and spiraled-sheet hybrid design

2.3 USV Target

A stainless steel (SS) target plate, shown in Figure 3(a), was used to evaluate the defect inspection capability of the UWT system under water and sodium. The target is 50.8 mm

× 50.8 mm (2″ × 2″) with 6.4 mm (1/4″) thickness. Letters and twelve slots with different width and depth were engraved on the plate. Each letter is 12.7 mm (1/2″) high, 3.2 mm (1/8″) wide and 1.6 mm (1/16″) deep. Each row of slots has the same width. From top to bottom, the width is 3 mm, 2 mm, 1 mm, and 0.5 mm. Each column of slots has the same depth. From left to right, the depth is 2 mm, 1 mm, and 0.5 mm. All slots have the same length of 9.5 mm. The slot with 0.5 mm width and 0.5 mm depth is the smallest feature patterned on the target.

To simulate the fuel-sub-assembly in an SFR and to evaluate the capability of component identification, another SS target is fabricated and shown in Figure 3(b). The target is a 50.8 mm × 50.8 mm (2″ × 2″) SS square plate with 12 pieces of SS tube and a mounting nut welded on. Each tube has an outer diameter (OD) of 9.4 mm (0.372″), an inner diameter (ID) of 6.9 mm (0.272″), and a height of 9.4 mm (0.370″). The mounting nut has an ID of 9.5 mm (0.375″) and a height of 8.4 mm (0.33″), which imitates a falling/loosing component among the fuel assembly.

Fig. 3. SS “USV” and “Tube” targets (size: 2″ × 2″, 50.8 mm × 50.8 mm) used to evaluate the UWT system (a) for defect inspection and (b) for components identification

2.4 Signal Processing

A graphical user interface (GUI) was developed under MATLAB® for data and image processing. The GUI is implemented modularly allowing one to easily update the existing functions (plugins) or create new algorithms that are independent of the core code.

The following features have been integrated into the developed GUI: 1) Flexibility to select gates (time windows) on the ultrasonic waveform; 2) Leading-edge follower to eliminate the effect of the misalignment between the target and UWT; 3) Baseline subtraction to remove background noise; 4) Running average to further increase S/N; 5) Raster offset to correct the possible offset introduced through scanning stage; 6) Animation segment to continuously monitor the RF signal change along the scanning route; 7) Dual display of TOF and intensity images with the corresponding line profiles at the selected position; 8) 3-D image presentation of the results.

3. Results and Discussions

3.1 UWT performance evaluation

The performance of our prototype UWT (152.4 mm / 6″) was compared with other three designs using threaded rod (152.4 mm / 6″), bundled rod (139.7 mm / 5.5″), and spiraled-sheet rod (146.1 mm / 5.75″), respectively. The evaluation was conducted in water by using a 5 MHz longitudinal transducer (12.7 mm / 0.5″ diameter, Aero Tech). The transducer was excited with a high-voltage pulser/receiver (Panametrics model 5058PR) with 200 V pulse voltage and 40 dB signal gain. An SS metal plate (50.8 mm × 50.8 mm / 2″ × 2″) with smooth surface was used as the target. Fig. 4 shows the comparison of target reflections.

Fig. 4. Evaluation of the internal and target ultrasonic signals using (a) threaded rod WG, (b) bundled rod WG, (c) spiraled-sheet rod WG, and (d) ANL prototype WG

From Fig. 4 (a)-(d), are the results of threaded rod, bundled rod, spiraled-sheet rod, and ANL prototype, respectively. In summary, both the threaded and bundled rods have poor S/N because of spurious signals from mode conversion. The spiraled-sheet design provides a better S/N over a wide time window for the target reflection. However, its applications are limited by a low percentage of energy transmitted into water or liquid sodium.

Under the same test conditions, our prototype UWT provides the best S/N with attenuation about 0.8 dB/m. The prototype UWT demonstrates high detection sensitivity with minimal background noise by effectively reducing spurious echoes and mode conversions.

3.2 USV performance evaluation – In water

The USV system was first evaluated under water at room temperature using the same target for defect detection. In the experiment, the scanning size is 50.8 mm × 50.8 mm (2″ × 2″) to cover the whole target, with a resolution of 50 pixel/in. The target plate is placed 34 mm (1.34″) away, which is at the nominal focal point of the waveguide in water. Images from TOF and intensity results are shown in Figure 5(a) and (b), respectively. The smallest feature, slot with 0.5 mm width and 0.5 mm depth, can be clearly resolved in the intensity image.

Fig. 5. Under-water imaging results of defect inspection (scanning area: 2″ × 2″, 50.8 mm × 50.8 mm): (a) TOF image and (b) intensity image

To evaluate the performance of the USV system for component identification, a water test was employed first at room temperature using the tube target. Experiment settings are the same as those in defect inspection tests. Images from TOF and intensity results are shown in Figure 6(a) and (b), respectively. Small features, like the welding points can be clearly identified. Because of the updates of our current test facility, the evaluation of the USV system for component identification in sodium will be carried out and reported in the future.

Fig. 6. Under-water imaging results of component identification (scanning area: 2″ × 2″, 50.8 mm × 50.8 mm): (a) TOF image and (b) intensity image

3.3 USV performance evaluation – In sodium

The under-sodium imaging was carried out at various temperatures and target distances. Results of 12″ WG have been reported [17, 18]. Figure 7 shows the results of 18" WG at 150°C (310 °F), while the target plate is 25.4 mm (1″) away. The scanning size is 25.4 mm × 25.4 mm (1″ × 1″) with a resolution of 50 pixel/in. Figure 7(a) shows the reflected acoustic signal from the target at the crossing point shown in TOF and intensity images. Figure 7(c) and (d) shows the TOF and intensity images respectively. The corresponding scanning area is highlighted in Figure 7(d).

Fig. 7. Under-sodium imaging results (18″ WG, 310 °F, 1″ separation, scanning area: 1″ × 1″, 25.4 mm × 25.4 mm): (a) acoustic signal reflected from target at the crossing point; (b) TOF image; (c) intensity image; (d) corresponding scanning area on the target

Two reflected echoes can be identified in Figure 7(a). The first and second echoes are generated by the signal reflected from the front surface and the bottom part of letter “V”, respectively. The depth of letter “V” is 1.6 mm, which introduces a 1.33 μs delay of TOF. This difference agrees well with the calculation based on the depth that further confirms that the second echo is caused by the engraved feature. Both echoes were used to generate TOF and intensity images, as shown in Figure 7(b) and (c). From these images, letters “S”, “V”, slot with 1 mm depth and 3 mm width, slot with 0.5 mm depth and 3 mm width, and part of slot with 0.5 mm depth and 2 mm width are clearly identified. These results manifest that our 457.2 mm (18″) prototype waveguide is able to achieve a vertical resolution of 0.5mm and a lateral resolution of 1 mm in molten sodium.

Fig. 8. Under-sodium imaging results (18″ WG, 650 °F, 1.25″ separation, scanning area: 1″ × 1″, 25.4 mm × 25.4 mm): (a) TOF image and (b) intensity image

Measurements at different temperatures and target separations were also conducted. Figure 8 shows the results taken at 650 °F using a 457.2 mm (18″) WG. The scanning area is 25.4 mm × 25.4 mm (1″ × 1″) with the same resolution as in Figure 7. The target is 31.8 mm (1.25″) away. Because of the adjustment of the set-up during the heating, the location is not exactly the same as that shown in Figure 7. Letter “V”, part of letter “S”, slot with 0.5 mm depth and 3 mm width, and the edge of target plate are clearly shown in both time-of-flight and intensity images. Furthermore, comparison between the images of letter “V” demonstrates that a slight distance variation between target and WG would not affect the performance of our USV system.

4. Conclusions

We have successfully developed a bench scale sodium test facility. The USV system based on UWT was evaluated in water at room temperature and molten sodium up to 650°F. The ultrasonic waveguide imaging system demonstrates the capability of detecting defects with 1mm in width and 0.5mm in depth under sodium, which is comparable with the required resolution using optical methods.

Our USV system has demonstrated a great potential for in-service inspection in high temperature and highly corrosive environments, such as the reactor core of an SFR. Besides that, the developed system also shows promising applications in other hostile environments.

References

[1] Generation IV Nuclear Energy Systems Ten-Year Program Plan, Idaho National Laboratory, 2007.

[2] Cinotti L, Fazio C, Knebel J, Monti S, Abderrahim HA, Smith C, Suh K. LFR "Lead-Cooled Fast Reactor". FISA 2006, Luxembourg, EU, 2006, UCRL-CONF-221396.

[3] Babelot JF, Fiorini GL, Abram T. Hill R, Hahn D, Ichimiya M, Lennox T, Mizuno T. SFR: Sodium-cooled Fast Reactor. Proc. Conf. Research and Training in Reactor Systems, Luxembourg, EU, 2006; pp 226-247.

[4] Williams DF, Toth LM, Clarno KT. Assessment of Candidate Molten Salt Coolants for the Advanced High-Temperature Reactor (AHTR). ORNL/TM-2006/12.

[5] Baqué SF. Review of In-Service Inspection and Repair Technique Developments for French Liquid Metal Fast Reactors. Nuclear Technology 2005;150: pp.67-78,.

[6] R. D. Watkins, M. O. Deighton, A. B. Gillespie and R. B. Pike, "A Proposed Method for Generating and Receiving Narrow Beams of Ulrasound in the Fast Reactor Liquid Sodium Environment" Ultrasonics 1982;20: pp. 7-12.

[7] Ultrasonic Imaging Allows Regular Inspection of Fast Reactor Core through Liquid Sodium Coolant. NDT International 1983;16: pp. 97-101.

[8] Barrett LM, McKnight JA, Fothergill JR. Ultrasonic Viewing in Fast Reactors. Phys. Technol. 1984;15: pp. 308-314.

[9] Karasawa H, Izumi M, Suzuki T, Nagai S, Tamura M, Fujimori S. Development of Under-sodium Three-dimensional Visual Inspection Technique Using Matrix-arrayed Ultrasonic Transducer. J. of Nuclear Science and Technology 2000;37: pp. 769-779.

[10] Rehman AU, Jen CK, Ihara I. Ultrasonic Probes for High Temperature Immersion Measurements. Meas. Sci. Technol. 2001;12: pp. 306-312.

[11] Joo YS, Lee JH. Ultrasonic Waveguide Sensor Using a Leaky Lamb Wave for Under-Sodium Viewing. Review of Progress in Quantitative Nondestructive

Evaluation, edited by D. O. Thompson and D. E. Chimenti, AIP Conference Proceedings, American Institute of Physics, 2009;29: pp. 1013-1020

[12] Ying SP, Scott CC. Concepts for General Purpose Under Sodium Scanning Systems. Atomic Power Development Associates Report No. APDA-179, 1965.

[13] Scott CC, Huebotter PR, Callen RC. Potential Applications for an Under-Sodium Ultrasonic Scanning Device. Atomic Power Development Associates Report No. APDA-205, 1967.

[14] Ord RN, Smith RW. Development of an Under-Sodium Ultrasonic Scanner for in-Reactor Surveillance. Hanford Engineering Development Laboratory Report No. HEDL-TME 72-91, 1972.

[15] ASME Section XI: Rules for In-service Inspection of Nuclear Power Plant Components, ASME Standard, 2010.

[16] Sheen S-H, Chien H-T, Wang K, Lawrence WP, Engel DM, Raptis AC. Ultrasonic Array Waveguide Transducer for Under Sodium Viewing. ANL Invention Report, 2010.

[17] Chien H-T, Wang K, Lawrence WP, Engel DM, Miranda D, Sheen S-H. Ultrasonic Waveguide Transducer for Under-Sodium Viewing. Proceeding of 7th American Nuclear Society International Topic Meeting 2010, American Nuclear Society.

[18] Wang K, Chien H-T, Lawrence, WP, Engel, D, Sheen S-H. Development of a Novel Ultrasonic Waveguide Transducer for Under-Sodium Viewing. Review of Progress in Quantitative Nondestructive Evaluation, edited by D. O. Thompson and D. E. Chimenti, AIP Conference Proceedings 1335, American Institute of Physics, 2010;30: pp. 1655-1662.

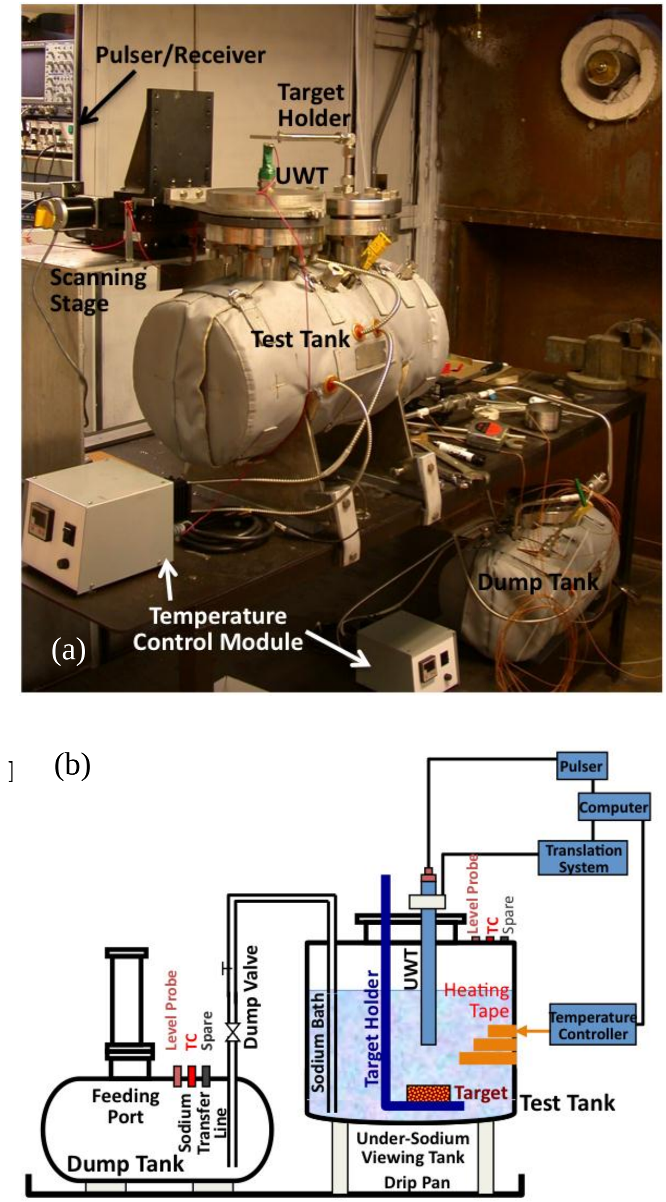

Fig. 1. Under-sodium viewing system: (a) experimental setup and (b) schematic drawing

Fig. 2. ANL 12˝ (304.8 mm) prototype UWT with bundle-rod and spiraled-sheet hybrid design

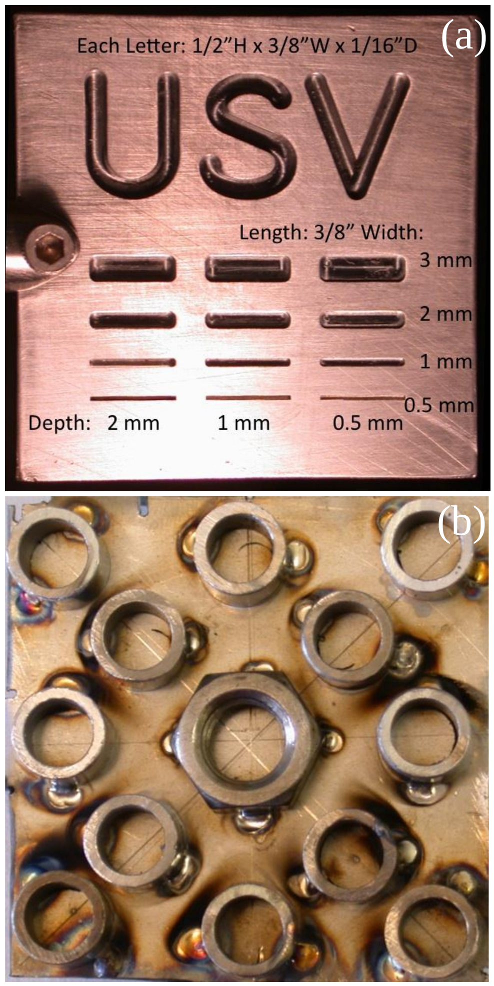

Fig. 3. SS “USV” and “Tube” targets (size: 2″ × 2″, 50.8 mm × 50.8 mm) used to evaluate the UWT system (a) for defect inspection and (b) for components

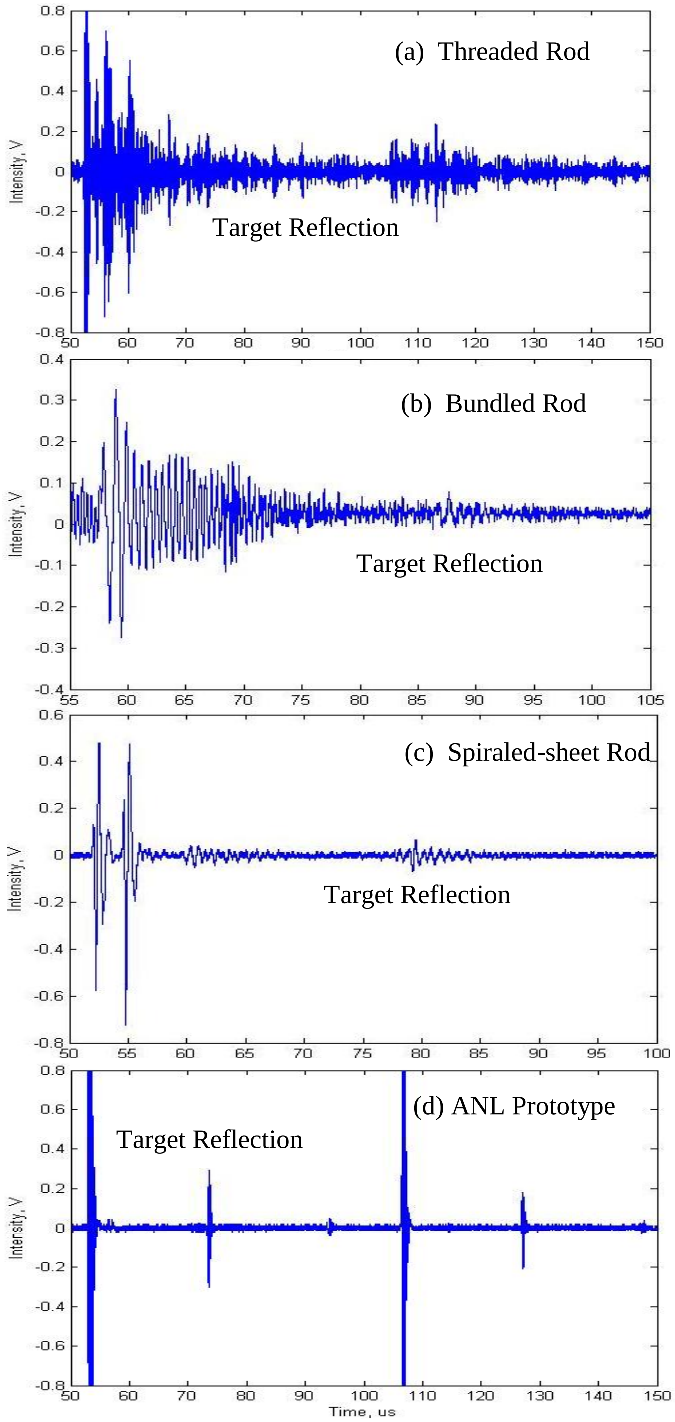

Fig. 4. Evaluation of the internal and target ultrasonic signals using (a) threaded rod WG, (b) bundled rod WG, (c) spiraled-sheet rod WG, and (d) ANL prototype WG

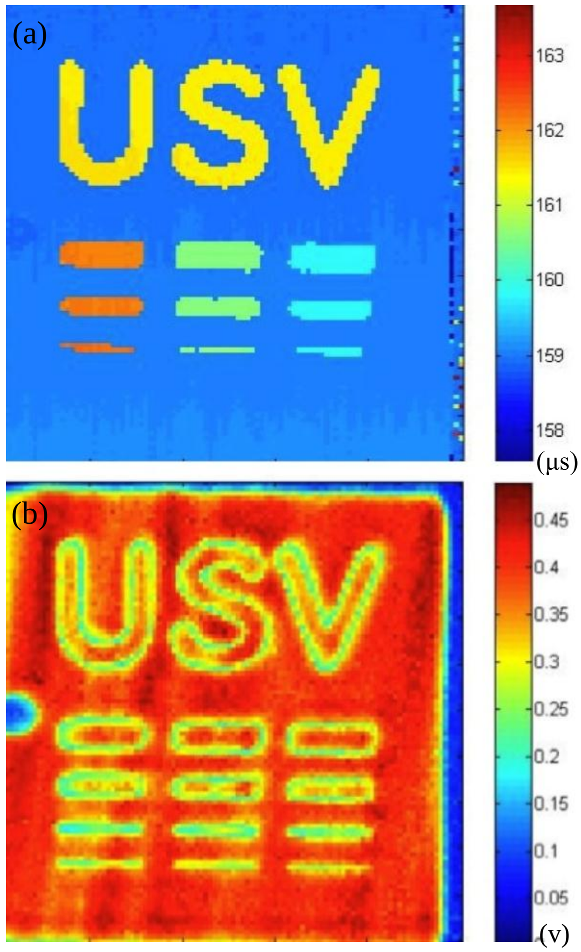

Fig. 5. Under-water imaging results of defect inspection (scanning area: 2″ × 2″, 50.8 mm × 50.8 mm): (a) TOF image and (b) intensity image

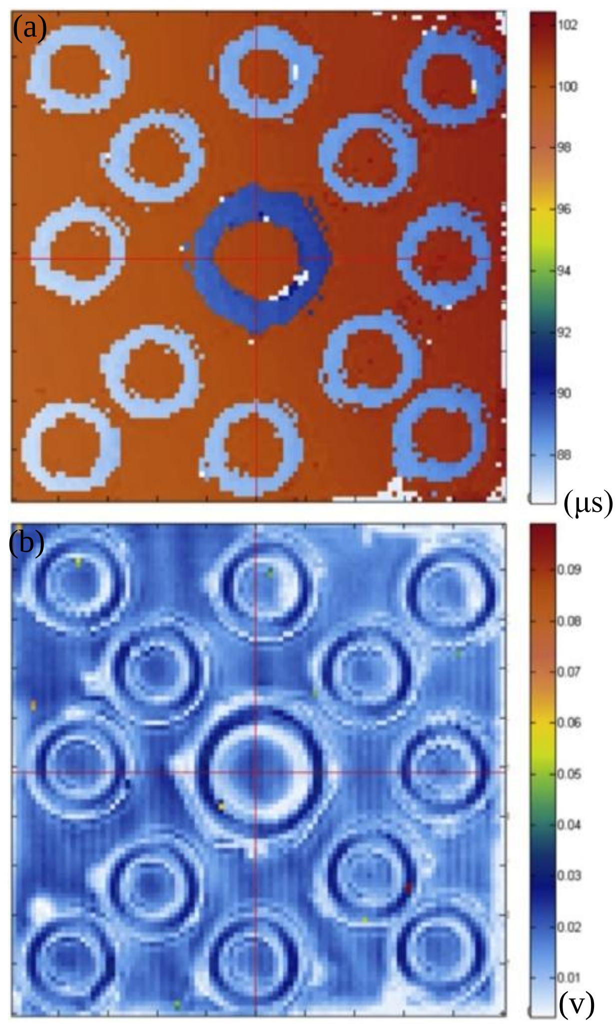

Fig. 6. Under-water imaging results of component identification (scanning area: 2″ × 2″, 50.8 mm × 50.8 mm): (a) TOF image and (b) intensity image

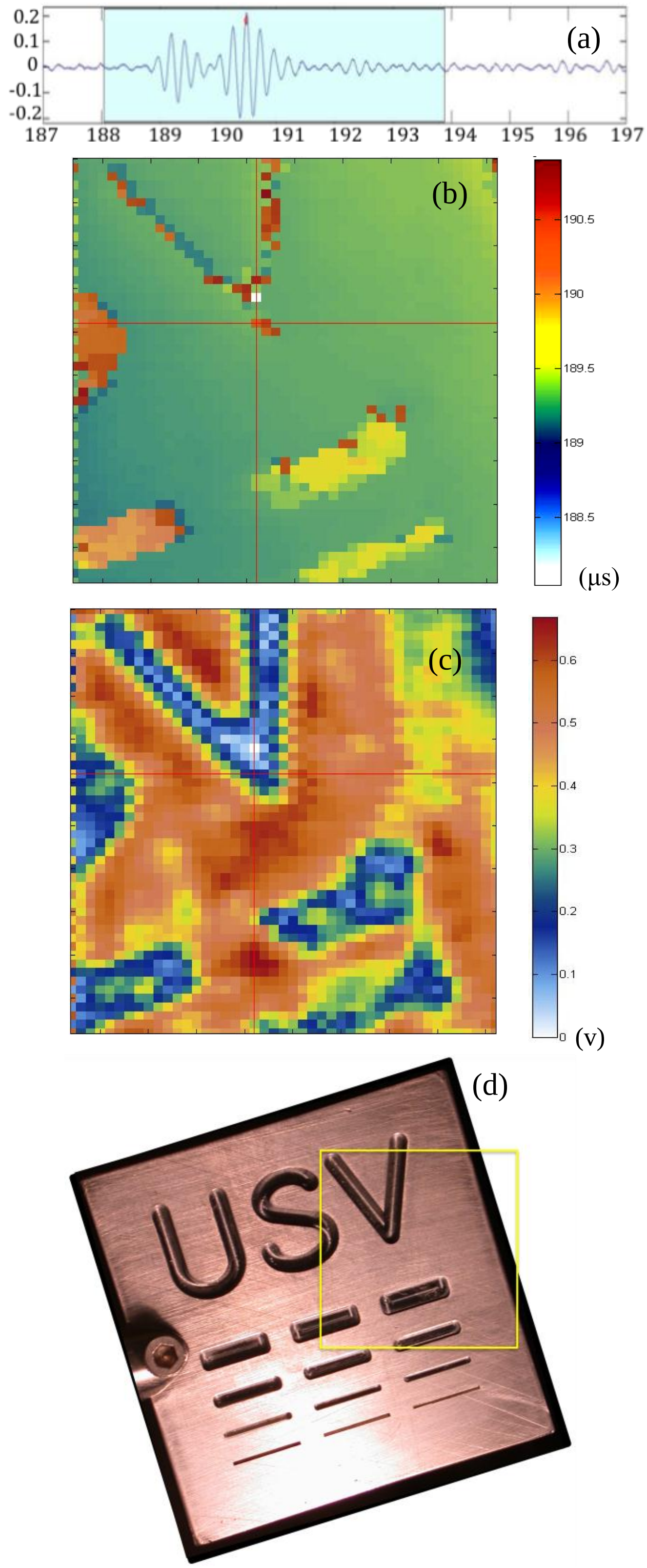

Fig. 7. Under-sodium imaging results (18″ WG, 310 °F, 1″ separation, scanning area: 1″ × 1″, 25.4 mm × 25.4 mm): (a) acoustic signal reflected from target at the crossing point; (b) TOF image; (c) intensity image; (d) corresponding scanning area on the target

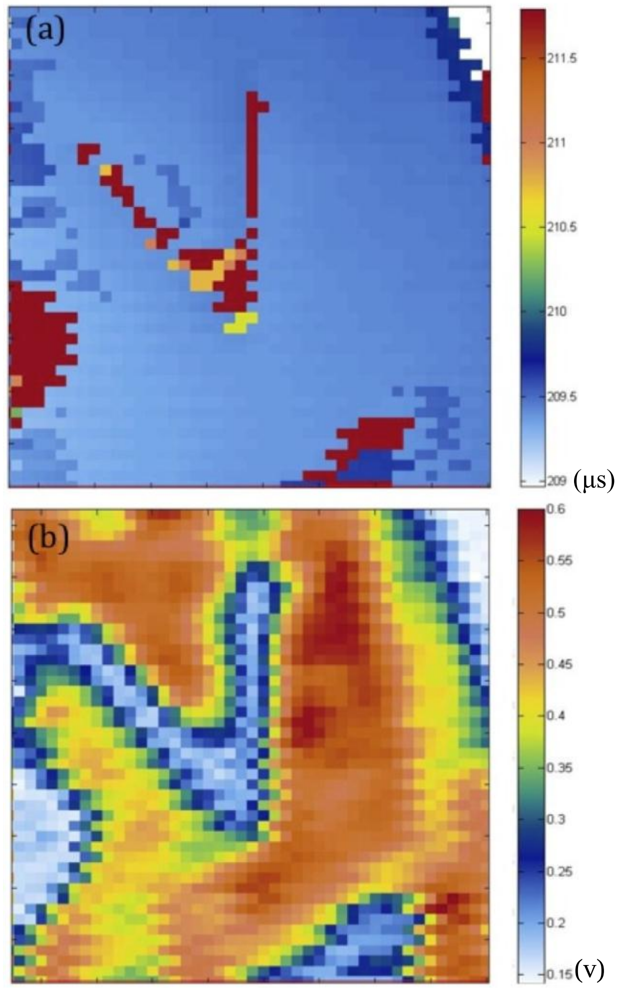

Fig. 8. Under-sodium imaging results (18″ WG, 650 °F, 1.25″ separation, scanning area: 1″ × 1″, 25.4 mm × 25.4 mm): (a) TOF image and (b) intensity image